Short-wavelength ablation of molecular solids: pulse duration and wavelength effects

Libor Juha
Michal Bittner
Dagmar Chvostová
Josef Krása
Michaela Kozlová
Miroslav Pfeifer
Jiri Polan
Ansgar R. Präg
Bedrich Rus
Michal Stupka
Academy of Sciences of the Czech Republic
Institute of Physics
Na Slovance 2, 182 21 Prague 8
Czech Republic
E-mail: juha@fzu.cz

Josef Feldhaus
HASYLAB/DESY
Notkestrasse 85
D-22603 Hamburg, Germany

Vit Létal
Zdenek Otcenasek
Czech Technical University in Prague
Faculty of Nuclear Sciences and Physical Engineering
Brehova 7, 115 19 Prague 1
Czech Republic

Jacek Krzywinski
Robert Nietubyc
Jerzy B. Pelka
Polish Academy of Sciences
Institute of Physics
Al. Lotników 32/46
PL-02-668 Warsaw, Poland

Andrzej Andrejczuk
University of Bialystok
Institute of Experimental Physics
Lipowa 41
PL-15-424 Bialystok, Poland

Ryszard Sobierajski
Warsaw University of Technology
Ul.Sw A. Boboli 8
PL-02-525 Warsaw, Poland

Leszek Ryc
Institute of Plasma Physics and Laser Microfusion
Ul. Hery 23, PL-00-908 Warsaw
Poland

Frederick P. Boody
Ion Light Technologies GmbH
Lessingstrasse 2c, 93077 Bad Abbach
Germany

Henryk Fiedorowicz
Andrzej Bartnik
Janusz Mikolajczyk
Rafal Rakowski
Military University of Technology
Ul. Kaliskiego 2, PL-00-908 Warsaw
Poland

Pavel Kubát
Academy of Sciences of the Czech Republic
J. Heyrovský Institute of Physical Chemistry
Dolejškova 3, CZ-18223 Prague 8
Czech Republic

Ladislav Pína
Martin Horváth
Reflex sro
Novodvorská 994, 142 21 Praha 4
Czech Republic

Michael E. Grisham
Georgiy O. Vaschenko
Carmen S. Menoni
Jorge J. Rocca
Colorado State University
NSF ERC for Extreme Ultraviolet Science and Technology
Department of Electrical and Computer Engineering
Fort Collins, Colorado 80523

Abstract. For conventional wavelength (UV-vis-IR) lasers delivering radiation energy to the surface of materials, ablation thresholds, ablation (etch) rates, and the quality of ablated structures often differ dramatically between short (typically nanosecond) and ultrashort (typically femtosecond) pulses. Various short-wavelength ($\lambda < 100$ nm) lasers emitting pulses with durations ranging from ~10 fs to ~1 ns have recently been put into routine operation. This makes it possible to investigate how ablation characteristics depend on pulse duration in the XUV spectral region. Four sources of intense short-wavelength radiation available in the authors' laboratories, including XUV and soft x-ray lasers, are used for the ablation experiments. Based on the results of the experiments, the etch rates for three different pulse durations are compared using the XUV-ABLATOR code to compensate for the wavelength difference. Comparing the values of etch rates calculated for nanosecond pulses with those measured for shorter pulses, we can study the influence of pulse duration on XUV ablation efficiency. The results of the experiments also show that the ablation rate increases while the wavelength decreases from the XUV spectral region toward x-rays, mainly due to increase of attenuation lengths at short wavelengths. [DOI: 10.1117/1.2037467]

Subject terms: laser materials modification; x-ray lasers; laser-induced damage; extreme ultraviolet; polymers.

Paper 04154R received Nov. 10, 2004; revised manuscript received Mar. 10, 2005; accepted for publication Mar. 30, 2005; published online Aug. 30, 2005. This paper is a revision of a paper presented at the SPIE Conference on Fourth Generation X-Ray Sources and Optics II, Aug. 2004, Denver, Colorado. The paper presented there appears (unrefereed) in SPIE Proceedings Vol. 5534.

1 Introduction

Although the decomposition of solid structures into tiny pieces induced by high-energy XUV/x-ray photons, result-

1537-1646/2005/$22.00

ing in material removal due to rapid evaporation of the low-molecular weight fragments, was first studied more than 20 years ago,[1–8] these processes were investigated only infrequently until now. Current research activities are not yet very extensive, although there are five strong sources of motivation to conduct systematic study in this field.

1. Estimating and minimizing damages to surfaces of highly irradiated XUV/x-ray optical elements developed and used for the guiding and focusing of short-wavelength laser beams, as well as those used for long-term irradiation with high repetition rate sources.[9–13]
2. Durability assessments of materials suggested for the first walls of inertial confinement fusion (ICF) reactors and optical elements exposed to intense XUV/x-ray radiation in a laser-plasma interaction chamber.[7,8]
3. Diffraction-limited ultrastructuring and patterning of solid surfaces for fabrication of microelectronic and micromechanical elements and devices.[7,8]
4. Determination of radiation field characteristics: imaging of spatial energy distribution in a focused beam ablatively imprinted on the irradiated material and determination of pulse energy content.[14,15]
5. Production of very dense plasmas with low electron temperatures, i.e., $T_e \sim 10$ eV.[16]

The XUV/x-ray sources used for material ablation emit at both low peak power (synchrotron radiation[2,6] and rotating anode[5] sources) and high peak power [free-electron lasers (FELs)[17–20] and various sources based on hot dense plasmas[1,3,4,8]]. With low peak power sources, materials are removed by photon-induced desorption of material components from the irradiated sample surface. Each XUV/x-ray photon carries enough energy to break any chemical bond. This energy is also usually higher than the cohesive energy of any crystal. Therefore, the photons absorbed in a near-surface region may create small fragments of a sample material, which are emitted into the vacuum. It is necessary to underline that in the case of low peak intensity irradiation, material is removed from the surface and a very thin near-surface layer only. Quite a different situation is expected if a high peak power source delivers a single high-energy pulse to the sample. The sample is then exposed to a high local dose of radiation (given by the energy content of the pulse and the absorption length of the radiation in the irradiated material) in a short period of time (given by the pulse duration), i.e., at a very high dose rate. This means that a large number of events that cause radiation-induced structural decomposition (i.e., polymer chain scissions, etc.), occurs almost simultaneously in a relatively thick layer of irradiated material. Since a portion of the radiation energy absorbed in the material will be thermalized, the sudden heating of the layer, which is also heavily chemically altered by the radiation, must be taken into account. The overheated, fragmented region of the sample represents a new phase, which tends to blow off into the vacuum. These particular processes, as well as specific features of short-wavelength ablation with respect to ablation induced by conventional UV-vis-IR sources, represent the subject of our research.

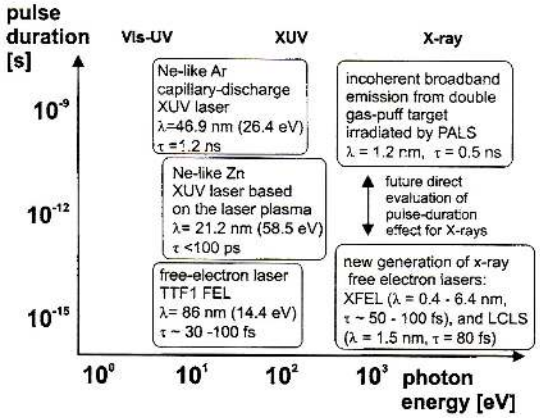

Fig. 1 Photon energy and pulse duration characteristics of the XUV and soft x-ray sources used in this study.

Ablation characteristics, i.e., thresholds, etch (ablation) rates, and ablated structure quality, often differ dramatically with conventional UV-vis-IR lasers, depending on whether the radiation energy is delivered to the material surface in either short (typically nanosecond) or ultrashort (typically femtosecond) pulses.[21–23] Does such a difference also exist for lasers operating in the XUV ($\lambda < 100$ nm) spectral region? This question can now be answered due to the availability of XUV lasers with pulse durations ranging from tens of femtoseconds to several nanoseconds.[24–28] These sources, which became available only recently, are promising tools for applications in the field of nanopatterning of solids, as they will enable the printing of features with dimensions comparable to the wavelength. A key advantage of XUV lasers for nanostructure fabrication is the unique combination of exceptionally short wavelength, high spatial coherence, and high peak power. High thresholds for material processing require XUV sources to deliver enough fluence and thus sufficiently high power to the irradiated surface area. Although noncoherent sources developed for XUV lithography can also pattern material surfaces at sub-10-nm resolutions, they cannot directly produce 3-D structures using only a few shots in a single processing step. Recently it has been demonstrated that intense XUV radiation can directly produce sub-100-nm structures quite easily. Grating-like structures [i.e., laser-induced periodic surface structures (LIPSS)] with spatial periods of about 70 nm have already been produced in amorphous carbon (a-C)[10,19] and poly(methyl methacrylate) (PMMA)[29] surfaces irradiated with FEL radiation at 98 and 86 nm, respectively.

Since the previously mentioned short-wavelength lasers emit at different wavelengths, we should also investigate the wavelength dependence of the ablation characteristics. To extend wavelength scaling to even shorter wavelengths of the x-ray spectral region, since no x-ray lasers were available, an incoherent ~1-keV source based on laser-produced Xe plasma[30] was used in this study. However, two x-ray FEL systems are currently under construction. At Stanford, the Linac Coherent Light Source (LCLS),[31] which will be tunable from 0.8 to 8keV, is expected to be available for users in late 2006. And in Hamburg, commis-

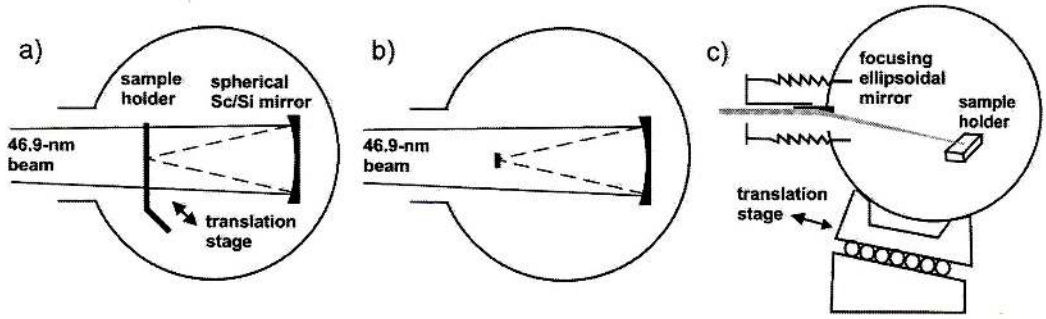

Fig. 2 (a) Top view and (b) side view of the focusing setup for the 46.9-nm beam of the Ne-like Ar laser,[34] and (c) schematic of the FELIS chamber and the focus setup realized at the FEL beam.

sioning of the XFEL facility,[32] which will be tunable from 0.2 to 12.4keV, is expected in 2012. These new sources provide strong motivation for studying material ablation and surface modification induced by intense keV radiation.

Four sources of intense short-wavelength radiation, including XUV and soft x-ray lasers, available in the authors' laboratories, have been used for investigating how ablation characteristics depend on pulse duration and wavelength in XUV/x-ray spectral regions. The first results from this project are presented in this work. The photon energy and pulse duration region covered by these sources are shown in Fig. 1.

2 Experiment

Focused beams from three XUV lasers of different types and output parameters have been used for irradiating various materials. The Ne-like Ar capillary-discharge laser[33] built and operated at the Colorado State University provided nanosecond pulses [full width at half maximum (FWHM) = 1.2 ns] of 46.9-nm radiation. Average pulse energy was ~130 μJ. The laser beam was focused onto the sample surface by a spherical Sc/Si multilayer-coated mirror with a measured reflectivity of ~30%. In the on-axis focusing layout [Figs. 2(a) and 2(b)] the sample holder blocks the central part of the incoming beam.[34] The ridges observed in the ablated spots are the result of the shadow produced by the sample holder.

The self-amplified spontaneous emission (SASE) free-electron laser at the TESLA Test Facility (TTF1 FEL[35]) in Hamburg, which operates between 80 and 120 nm, was tuned to a wavelength of 86 nm. The duration of TTF1-FEL pulses fluctuates between 30 and 100 fs. The beam was focused by an ellipsoidal multilayer mirror onto samples located in the free electron laser interaction with solids (FELIS)[17] interaction chamber, Fig. 2(c). The total energy of the laser pulses was determined using photodetectors illuminated by the radiation scattered from a gold wire placed in the incoming FEL beam. The wire is very important for collecting radiometric data for each pulse; however, the wavefront of the FEL beam is heavily perturbed by the wire. Fresnel diffraction patterns formed due to the wire are ablatively imprinted on the irradiated materials, making the crater profilometry more difficult.

Initial experiments with the focused beam of the Ne-like Zn soft x-ray laser[16,36] were conducted in November 2003. Lasing occurred at 21.2-nm on Ne-like ions in a zinc plasma generated by the high-power Prague Asterix Laser System (PALS) laser.[37] The pulse duration of the laser

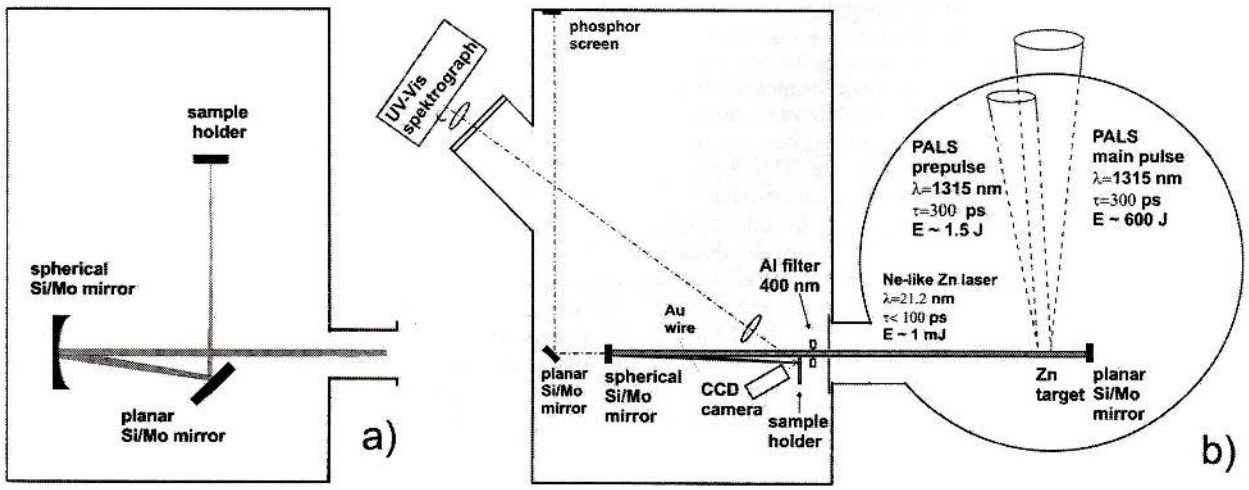

Fig. 3 (a) Two-mirror and (b) one-mirror focusing systems for the Ne-like Zn XUV laser beam at PALS.

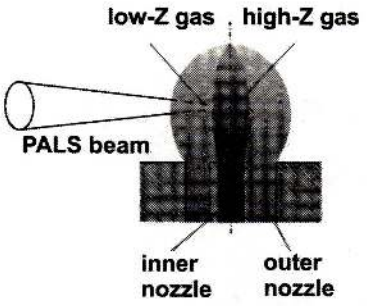

Fig. 4 Cross-sectional view of the double-gas-puff target.

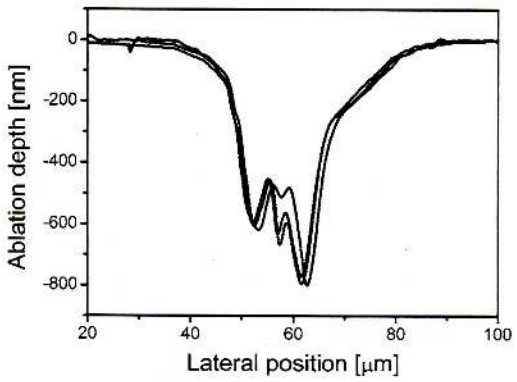

Fig. 5 Three independently measured profiles of a crater ablated in PMMA by a capillary-discharge XUV-laser beam.

emission was 80 to 90 ps. A system of spherical and planar Mo/Si-multilayer mirrors [see Fig. 3(a)] was used in the first experiments. However, reflection by the planar mirror caused significant pulse energy losses, so that the fluence fell to the vicinity of the ablation threshold at the material surface. During the second campaign held at PALS in May 2004, the simple one-reflection near-axis focusing layout, depicted schematically in Fig. 3(b), was used. Fluence at the sample surface was varied by the same method in all of the previously mentioned focusing schemes.

All three interaction chambers are equipped with a system for translating the sample along the XUV-laser beam optical axis with high accuracy with regard to the focal point. This allows control of the laser spot diameter on the sample. Thus, while the pulse energy and duration are kept constant, the laser fluence can be varied.

Hot dense Xe plasma produced by irradiating double-stream gas puff targets with the focused PALS NIR laser beam is a source of incoherent x-rays. The double-stream gas puff targets utilized two coaxial nozzles (see Fig. 4). An annular outer nozzle produced a hollow cylinder of He, suppressing sideways expansion of the Xe. Double-stream gas puffs have been shown to improve IR to XUV conversion efficiency compared to conventional single-stream gas puffs. Ion emission is suppressed by the outer gas envelope surrounding the plasma. The absence of ion current was verified using ion collectors. PMMA samples were placed at various distances to the source, each behind a mesh contact mask. For more details about the source and irradiation conditions, see Ref. 30.

Poly(methyl methacrylate) (PMMA) and polyimide (PI) sheets 1 mm thick (Goodfellow, United Kingdom) were cut into 2.0×5.0-mm^2 chips for the 46.9-nm laser experiments, and into 5.0×5.0-mm^2 chips for irradiation by the incoherent source. The same PMMA sheet, but fabricated into 13×32-mm^2 slabs, was irradiated with the FEL beam. For irradiation at 21.2 nm, 500-nm layers of 495-K PMMA were deposited on 5×5-mm^2 315-μm-thick silicon chips (Silson, United Kingdom). The surface quality of both purchased PMMA samples was good enough so that no additional surface treatment was needed. Poly (tetrafluorethylene) (PTFE) samples (Goodfellow) were fabricated the same way as the PMMA samples. The only differences were in their polishing and short-term contact with a silicon wafer at a temperature of 300°C. The irradiated surfaces were investigated using profilometry and atomic force microscopy (AFM) performed with an Alpha-Step 500 Surface Profiler (Tencor, USA) and a Dimension 3100 scanning probe microscope (SPM) driven by a NanoScope IV controller (Veeco, USA). The accuracy of finding the crater's center and the reproducibility of the profilometric measurement of ablation depth are illustrated in Fig. 5 for three independent scans of one crater. XUV radiation fluences were calculated from laser pulse energy and crater outer diameter.

3 Computer Simulation of XUV Ablation: XUV-ABLATOR Code

Computer simulation of XUV ablation may help in comparing ablation rates when XUV lasers emitting at different wavelengths are used. We would like to differentiate the unknown influences of different wavelengths (in our case 46.9, 21.2, and 86 nm) and different pulse widths (1.2 ns, 80 to 90 ps, and 30 to 100 fs, respectively) on the ablation process. The idea of our method is illustrated in Fig. 6(a). Nanosecond ablation in the XUV spectral region is simulated with the computer code XUV-ABLATOR. If the calculated values agree with the experimental results for nanosecond ablation at a wavelength of 46.9 nm [Fig. 6(a), top], we expect to obtain realistic predictions [Fig. 6(a), outer circle] of nanosecond ablation rates at other wavelengths (86 and 21.2 nm), where nanosecond sources are not available. Then the calculated values can be compared with results of experiments [Fig. 6(a), inner circle] carried out with femtosecond and picosecond pulses at 86 and 21.2 nm, respectively.

The ABLATOR code[38–40] was developed by Anderson in the middle 1990s for numerical simulation of ablation of the materials proposed for first walls of inertial confinement fusion (ICF) reactors, induced by broadband emission (~keV) from NOVA-driven hohlraum targets. The original ABLATOR is a thermomechanical 1-D hydrodynamic code. It uses a Lagrangian finite-difference approach, which means that the matter is divided into zones with fixed mass but variable size, position, and velocity. At each time step [see Fig. 6(b)], the code computes the energy deposited in each zone by radiation, the heat conducted from the immediately adjacent zones, and the energy due to stress in the material. The Mie-Grüneisen equation of state (EOS) provides a new pressure that is linear with zone internal energy

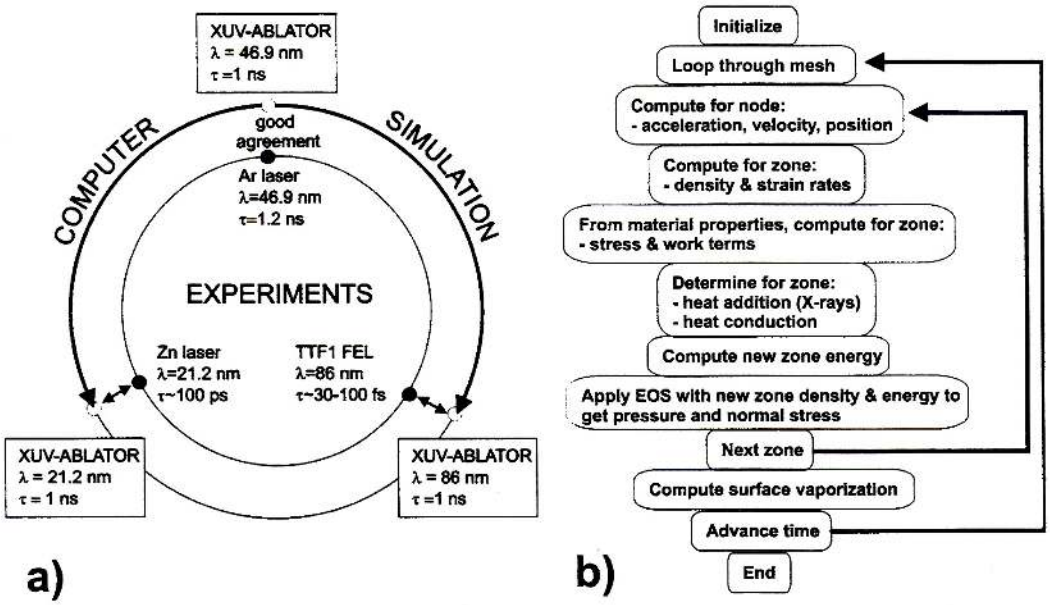

Fig. 6 (a) Scheme for evaluating pulse-length effects with radiation sources emitting at different wavelengths. The inner circle represents experimental results obtained with various XUV lasers and the outer circle indicates computer simulations with XUV-ABLATOR. (b) Flow chart of ABLATOR.[38]

and dependent on the zone density. Normal stress, given as the difference between the new pressure and the new deviatoric stress, controls further movement of a zone. This is done by calculating zone node movements from the hydrodynamic equation of motion, using normal stress in the zone and its neighbors. When the variables in all zones have been calculated, a new cycle starts. In every cycle, one zone is designated as the surface, for which the fraction of liquid and vapor is computed, assuming that only surface evaporation occurs. If the vapor/liquid fraction exceeds one, the next zone is designated as the surface. Cracking occurs if the tensile stress exceeds the critical value. For our simulations, the original ABLATOR was modified to model material ablation induced by XUV radiation, which has a much shorter attenuation length than x-rays. The modified code was renamed XUV-ABLATOR. Efficient absorption of XUV radiation results in a dramatic increase of temperature in the near-surface region of irradiated material, leading to difficulties with the calculation of thermal conduction, very high gradients decreasing simulation stability, etc. XUV-ABLATOR also takes into account radiation-chemical processes occurring in irradiated material. The most abundant degradation products of PMMA irradiated by a 25-eV electron beam are methyl methacrylate (MMA) and carbon dioxide (CO_2).[41] Therefore, the PMMA "vapors" in XUV-ABLATOR are composed of either MMA or CO_2. The upgrading of ABLATOR to simulate XUV ablation of molecular solids will be described in detail elsewhere.[42]

4 Results and Discussion

Figure 7(a) shows an optical micrograph of a PMMA sample exposed to five different fluences of 46.9-nm emission, increasing in the arrow direction. The six craters in each row were formed by accumulating 1, 2, 4, 8, 16, or 32 shots at each of the three fluences. The horizontal ridges observed in the ablated spots are the result of the shadow produced by the sample holder, which blocks part of the laser beam. The profiles shown in Fig. 7(b) were measured for the craters ablated by an accumulation of 32 XUV-laser shots. The average ablation rate reached a value of about 190 nm/pulse at the highest fluence (4.5 J/cm^2), while the crater shape remained almost unchanged. Only the central ridge, resulting from the holder shadow [see Figs. 2(a) and 2(b)], exhibits progressive erosion with increasing fluence, caused by material blow-off and aberration of the spherical mirror. The profiles presented in Fig. 7(b) indicate the character of the dependence of the maximum ablation depth on the laser fluence.

Figure 8(a) summarizes the fluence dependence of ablation rates calculated by XUV-ABLATOR and experimentally determined for a single-shot exposure and for 32 accumulated shots. Calculated values are in good agreement with those measured. Ablation rates, as well as their fluctuations, decrease with the accumulation of several pulses. As is well known, ablation is very sensitive to the energy of laser pulses, and even small fluctuations can dramatically influence the ablation rate. Thus, the observed difference between single- and multiple-shot experiments in ablation-rate-fluctuation levels can be explained by the shot-to-shot fluctuation of the laser output power. The observed decrease of ablation rates with increasing number of shots may occur for several reasons.[21] In addition to the reasons reported by Bäuerle for laser radiation of any wavelength, the radiation-chemical action of high-energy photons should be taken into account with short-wavelength lasers. The radiation-chemical changes in organic polymers involve two processes—chain scissions and cross-linking.

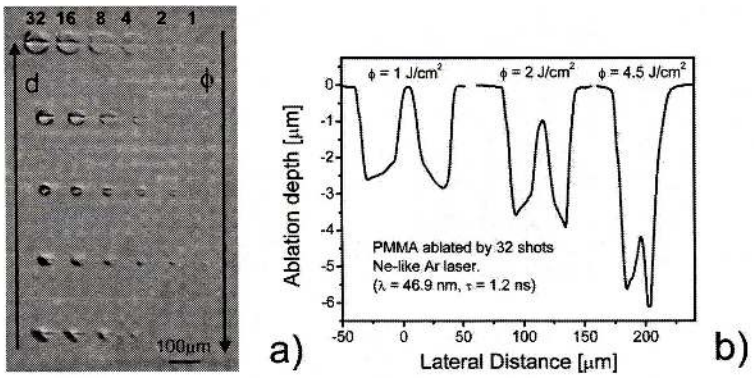

Fig. 7 (a) Optical micrograph of PMMA sample irradiated with 46.9-nm emission at five different fluences with an increasing number of laser shots (1...32). Fluence increases from top to bottom and the number of shots increases from right to left. (b) Profiles of the craters ablated in PMMA by 32 shots of 46.9-nm laser radiation at the first three fluences.

The latter can increase stability of the polymer and reduce ablation rate. Good agreement of the calculated ablation rates with both measured dependences for the ablation induced by nanosecond 46.9-nm pulses supports the usability of XUV-ABLATOR for the prediction of nanosecond ablation induced by nanosecond XUV pulses at other wavelengths, as suggested in Fig. 6(a).

It can be seen in Fig. 7 that PMMA ablation induced by nanosecond 46.9-nm pulses is very clean. The surface quality of irradiated and ablated material is very high. The AFM image in Fig. 8(b) confirms this finding. The crater has sharp edges without material expansion. Neither bubbles nor thermal damages can be seen at the surface of the crater or its rim. This indicates strong absorption of XUV-laser radiation in the material and testifies to a key role for non-thermal processes in XUV-laser ablation.

In the FELIS interaction chamber, PMMA was ablated by 86-nm ultrashort FEL pulses with durations fluctuating from 30 to 100 fs. 11 pulses were accumulated at an average fluence of 0.44 J/cm^2 to produce the crater whose Nomarski micrograph is presented in Fig. 9(a). Figure 9(b) shows the profiles of three craters ablated at three different fluences of FEL radiation. The measured ablation-rate values for 30- to 100-fs FEL pulses are shown in Fig. 10, together with the values calculated for nanosecond pulses of 86-nm radiation with XUV-ABLATOR. It is found that sub-100-fs pulses of 86-nm FEL radiation ablate PMMA at lower rates than predicted by simulation for nanosecond pulses at the same wavelength. Taking into account that the ablation occurs in the low-fluence regime, where the rate is controlled by attenuation length, it follows from the results summarized in Fig. 10 that the attenuation length of FEL radiation must be shorter than that derived from the linear absorption coefficient (10 nm for PMMA at 86 nm[43,44]). The absorption length is a key input parameter in the XUV-ABLATOR simulation for nanosecond pulses.

The difference may be explained if one assumes that absorption is enhanced for ultra-intense, ultra-short pulses.

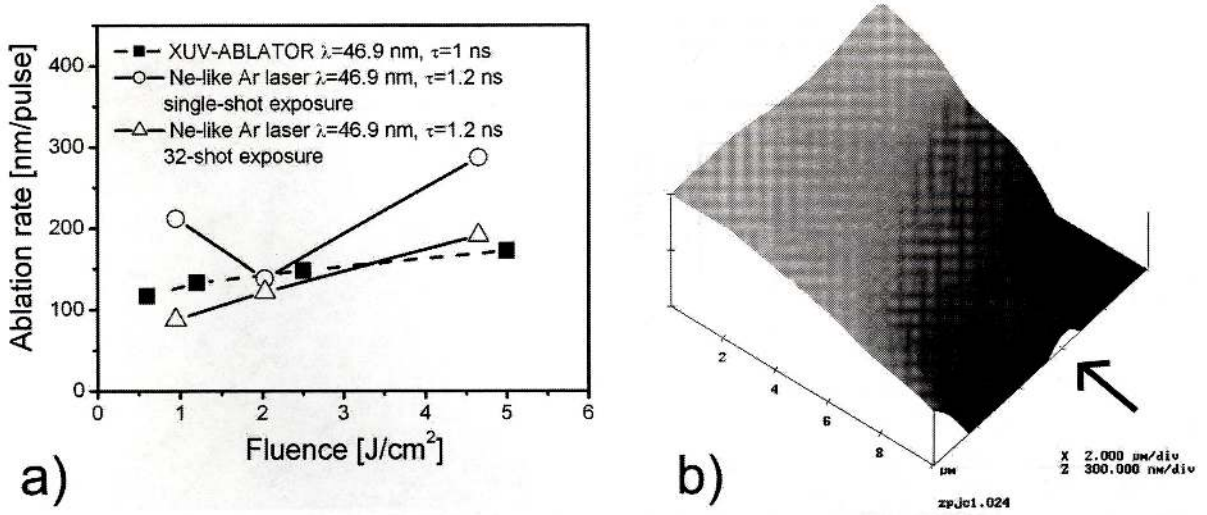

Fig. 8 (a) Fluence dependence of PMMA ablation rates calculated and measured for nanosecond pulses of 46.9-nm radiation. (b) AFM image of a part of the crater ablated in PMMA by four accumulated 46.9-nm laser pulses at a fluence of 3.3 J/cm^2. The ridge formed due to the sample-holder shadow is marked by the arrow.

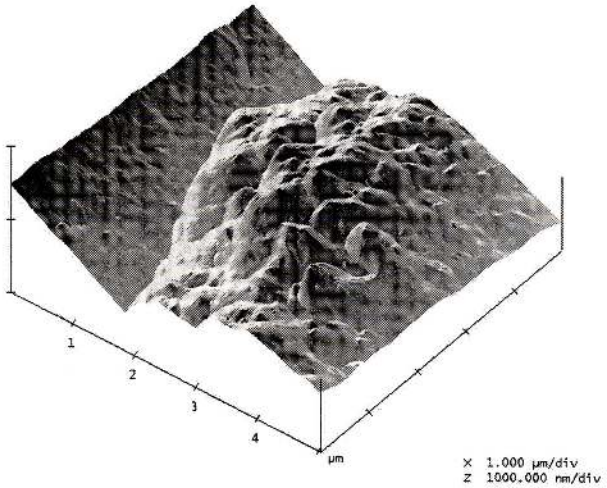

Fig. 12 AFM image (tapping mode, tilted sample) of PTFE surface damaged by six sub-100-ps pulses of 21.2-nm laser radiation focused into a sub-100-μm spot.

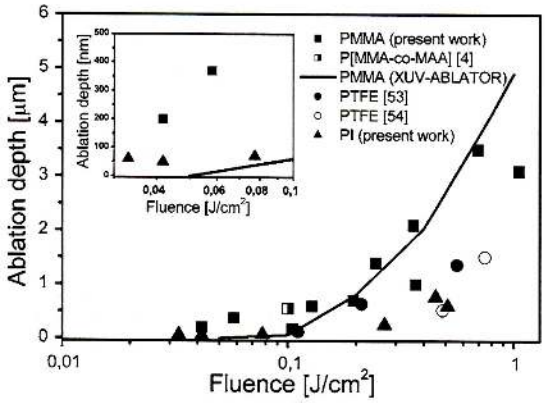

Fig. 14 Ablation of PMMA and PI induced by a single shot of incoherent 1-keV radiation emitted from a Xe-He gas-puff target irradiated with 0.5-kJ pulses of NIR laser radiation at the PALS facility. The attenuation lengths of 1.24-nm radiation are 3.0 and 2.5 μm in PMMA and PI, respectively. The solid line represents the etch rate of PMMA for 0.5-ns pulses of ~keV radiation, calculated with XUV-ABLATOR. Some values measured for P(MMA-co-MAA) and PTFE by other groups[4,53,54] are also shown for comparison.

veloped a single-reflection scheme [Fig. 3(b)] where the fluence level of ~0.1 J/cm^2 needed for efficient ablation of PMMA can be easily reached. Figure 13(a) shows profiles of two craters created in this setup by independent single soft x-ray laser pulses filtered by 400-nm aluminum foil, and that of a crater ablated by an unfiltered single pulse of the laser. Since the filter's transmission at 21.2 nm is about 50%, this crater was created at two-fold higher fluence than the other two craters. The ablation depths determined in the ablation experiment with sub-100-ps pulses of 21.2-nm radiation also seem to be reduced [factor of 2 to 3; see Fig. 13(b)] with respect to those calculated by XUV-ABLATOR for nanosecond pulses. However, the reason for this effect should be different than that discussed earlier for sub-100-fs pulses of 86-nm radiation. Attenuation length shortening is unlikely for sub-100-ps (i.e., lower intensity) pulses of 21.2-nm radiation, because strong nonlinear interaction of 58.5-eV photons is rather unlikely at intensities around 10 GW/cm^2. Explanation of the observed etch-rate reduction can be provided by the existence of a dose-rate region, where cross-linking of the PMMA chains competes efficiently with degradation of the chain into low-molecular weight products.[51] Development of a computer code for simulating PMMA ablation by sub-100-ps pulses of 21.2-nm radiation that includes this radiation-chemical effect is underway at the authors' laboratories.

Figure 14 compares the ablation rates of PMMA irradiated by broadband, ~keV x-rays emitted from hot dense Xe plasma[30,52] with those for PI irradiated under the same conditions. These results are also compared to published results from other groups for poly(methyl methacrylate-co-meth-acrylic acid) [P(MMA-co-MAA)][4] and PTFE[53,54] using similar radiation sources. Figure 14 clearly demonstrates that the micrometer ablation rate level for PMMA is reached at a fluence of 0.2 J/cm^2, and computer simulation

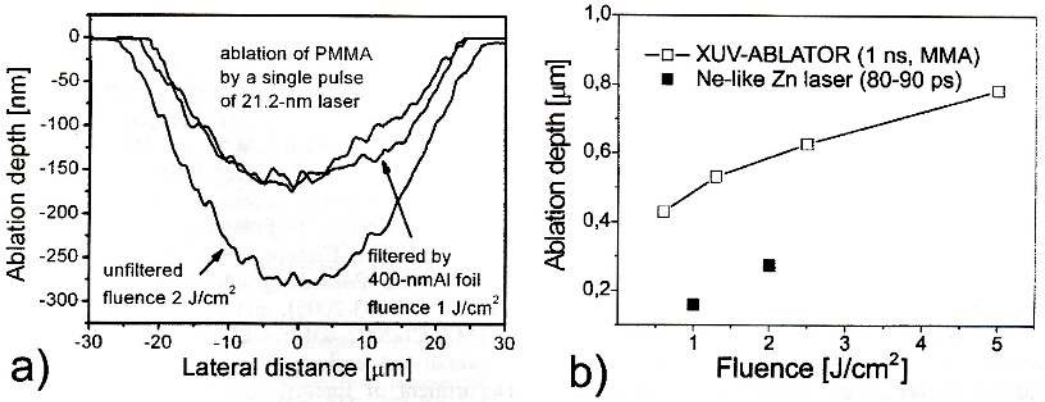

Fig. 13 (a) Profiles of three craters ablated in PMMA by a focused beam of Ne-like Zn XUV laser. The PMMA sample was irradiated at different places by two single shots filtered by 400-nm Al foil with transmission of about 50% at 21.2 nm and by one unfiltered shot. (b) Comparison of the ablation rates determined from the crater depths with that calculated by XUV-ABLATOR (MMA is considered as an evaporating product of PMMA radiolysis) for 1-ns pulses of 21.2-nm radiation.

of the ablation carried out with the XUV-ABLATOR code fits the experimental data very well. The simulation results are almost identical for both of the evaporating molecules considered, MMA and CO_2. Figure 14 shows only the results for CO_2.

Comparison of the ablation data presented in Figs. 7–10, 13, and 14 for XUV radiation and x-rays, respectively, leads to the conclusion that there is at least 1 order of magnitude difference in ablation rates between these two spectral regions due to the increase of attenuation length with decreasing wavelength. At the short wavelengths and low fluences, we also see a significant difference in ablation rates of particular polymers, which is in contrast to their XUV-ablation behavior.[55] The difference in attenuation lengths of 1-keV radiation in PMMA and PI is not large enough to explain the observed reduction of PI x-ray ablation efficiency with respect to PMMA. Differences in radiation-chemical and thermomechanical properties of the polymers must be taken into account. PI is well known as a material that exhibits high resistance to ionizing radiation and heat treatment. Since the thermal stability of both polymers is quite high, the higher ablation rate of PTFE compared to PI could testify to an indispensable contribution of radiation stability. However, such qualitative comparisons could be misleading, thus further computer simulations are needed to solve this problem. Figure 14 demonstrates the compatibility of our PMMA data[30] with previously measured x-ray ablation rates in P(MMA-co-MAA),[4] although radiation stability of the copolymer is in general lower than that of PMMA.[56]

If we compare our x-ray ablation data to that published for PTFE by Lawrence Livermore National Laboratory,[53,54] we see that PTFE ablation efficiency is also reduced with respect to our PMMA data. We can account for the significantly shorter attenuation length of 1-keV radiation in PTFE (about 1 μm) with respect to PMMA (also to PI) within the model of material ablation as a simple threshold process in which the ablation rate d at a fluence Φ is controlled by a threshold fluence Φ_{th} and the effective absorption coefficient α of the material:

$$d = 1/\alpha \cdot \ln(\Phi/\Phi_{th}). \quad (1)$$

The observed tendency of PTFE ablation efficiency reduction would make good sense for the data taken from Ref. 53 (full circles in Fig. 14), although an x-ray source with a different spectrum was used in LLNL than at PALS. However, both PTFE data[53,54] in Fig. 14 (full and open circles) seem to indicate a comparable or higher fluence position of the ablation threshold in PTFE than in PMMA, which is in contrast to the arguments presented in this paragraph and before for the PTFE irradiated by 21.2-nm radiation. This discrepancy, in principle, can be explained by a failure of the threshold concept in short-wavelength ablation (see the inset in Fig. 14), where significant ablation occurs well under the predicted threshold. This behavior results from the ability of even a single XUV/x-ray photon to break any chemical bond and deliver enough energy to overcome the cohesive energy of any crystal. Another explanation would be provided by the expansion behavior of PTFE irradiated by XUV/x-rays.[48] The material removed by softer radiation from the near-surface layer can be replaced by the material expanded due to the exposure of deeper sample levels to more penetrating, harder radiation. For the study of short-wavelength induced ablation and surface modification, coherent XUV/x-ray sources have the advantage of monochromaticity over incoherent laser-plasma based XUV/x-ray sources that always emit several energy groups of photons. However, in the keV region, coherent sources that allow single-shot experiments to be conducted are not yet available.

5 Conclusions

Efficient ablation (~10 to 100 nm/pulse), induced by nanosecond, picosecond, and femtosecond XUV lasers, is observed in PMMA, in complementary fluence regimes. The PMMA ablation efficiencies for lasers emitting pulses of various durations at different wavelengths can be compared indirectly through computer simulation of ablation induced by nanosecond pulses, using the XUV-ABLATOR code. First results suggest slightly enhanced absorption of ultra-intense XUV-FEL radiation in this organic polymer. The etch rate for sub-100-ps pulses of XUV laser radiation is also slightly reduced with respect to the values calculated for nanosecond pulses. However, this reduction cannot be explained in the same way as with ultra-fast XUV beams, because of the higher photon energy and lower intensity in the picosecond EUV beam. Surface quality of ablated materials is very high for every pulse duration. Craters with sharp edges, without bubbles or thermal damage, testify to the key role of nonthermal processes in XUV-laser ablation. Our initial XUV experiments do not show the dramatic difference between ablation of organic polymers with short and ultrashort pulses that is seen in UV-vis-IR. Short pulses of intense ~keV radiation emitted from laser-produced Xe plasmas induce PMMA removal at ~μm/pulse ablation rates. This is due to the larger attenuation lengths of x-ray radiation in PMMA, which is ~1 μm, compared to ~10 nm for XUV. In the x-ray region we also see a difference in ablation behavior of various organic polymers, which is often hard to distinguish at longer wavelengths, i.e., in the XUV region.

Acknowledgments

This work was partially funded by the EU Transnational Access to Research Infrastructures (grant HPRI-00108), by the National Research Centers (Project LN00A100), from program INGO (Grants LA055 and 1P2004LA235), by the Czech Academy of Sciences (Grant A1010014), by the Ministry of Scientific Research and Information Technology of the Republic of Poland (grant number 3 T08C 002 27), by the State Committee for Scientific Research of the Republic of Poland (grant number 72/E-67/SPB/5.PR UE/DZ 27/2003-2005), and by the European Commission (G1MA-CI-2002-4017; CEPHEUS). The Colorado State University researchers acknowledge the support of the U.S. Department of Energy, Chemical Sciences, Geosciences, and Biosciences Division of the Office of Basic Energy Sciences, and partial support of the Engineering Research Centers Program of the National Science Foundation under NSF Award Number EEC-0310717.

References

1. Y. M. Aleksandrov, K. A. Valiev, L. V. Velikov, S. D. Dushenkov, A. V. Mitrofanov, A. M. Prokhorov, and M. N. Yakimenko, "Photoetching of polymer foils induced by soft X-rays," *Pis'ma Zh. Tekh. Fiz.* **8**(10), 577–579 (1982).
2. S. Ichimura, M. Hirata, H. Tanino, N. Atoda, M. Ono, and K. Hoh, "Direct engraving on positive resist by synchrotron radiation," *J. Vac. Sci. Technol. B* **1**(4), 1076–1079 (1983).
3. B. Yaakobi, H. Kim, J. M. Soures, H. W. Deckman, and J. Dunsmuir, "Submicron x-ray lithography using laser-produced plasma as a source," *Appl. Phys. Lett.* **43**(7), 686–688 (1983).
4. V. A. Boiko, A. Y. Vainer, S. A. Kireeva, V. F. Limanova, I. Y. Skobelev, A. Y. Faenov, and S. Y. Khakhalin, "Photoetching of positive resists by intense x-ray pulses from a laser plasma," *Zh. Tekh. Fiz.* **53**(7), 1402–1403 (1983).
5. E. M. Lehockey, I. Reid, and I. Hill, "Physical and chemical aspects of PMMA vapour development," *Nucl. Instrum. Methods Phys. Res. B* **46**(1-4), 364–368 (1990).
6. Y. Zhang, "Synchrotron radiation direct photo-etching of polymers," *Adv. Polym. Sci.* **168**, 291–340 (2004).
7. L. Juha, "Materials ablation with soft x-rays," *Čs. Čas. Fyz.* **50**(2), 110–118 (2000).
8. L. Juha, J. Krása, A. Präg, A. Cejnarová, D. Chvostová, K. Rohlena, K. Jungwirth, J. Kravárik, P. Kubeš, Y. L. Bakshaev, A. S. Chernenko, V. D. Korolev, V. I. Tumanov, M. I. Ivanov, A. Bernardinello, J. Ullschmied, and F. P. Boody, "Ablation of poly(methyl methacrylate) by a single pulse of soft x-rays emitted from Z-pinch and laser-produced plasmas," *Surf. Rev. Lett.* **9**(1), 347–352 (2002).
9. J. Kuba, A. Wootton, R. M. Bionta, R. Shepherd, E. E. Fill, T. Ditmire, G. Dyer, R. A. London, V. N. Shlyaptsev, J. Dunn, R. F. Smith, S. Bajt, M. D. Feit, R. Levesque, and M. McKernan, "X-ray optics research for free electron lasers: study of material damage under extreme fluxes," *Nucl. Instrum. Methods Phys. Res. A* **507**(1,2), 475–478 (2003).
10. B. Steeg, L. Juha, J. Feldhaus, S. Jacobi, R. Sobierajski, C. Michaelsen, A. Andrejczuk, and J. Krzywinski, "Total reflection amorphous carbon mirrors for vacuum ultraviolet free electron lasers," *Appl. Phys. Lett.* **84**(5), 657–659 (2004).
11. M. Grisham, G. Vaschenko, C. S. Menoni, J. J. Rocca, Y. P. Pershyn, E. N. Zubarev, D. L. Voronov, V. A. Sevryukova, V. V. Kondratenko, A. V. Vinogradov, and I. A. Artioukov, "Damage to extreme-ultraviolet Sc/Si multilayer mirrors exposed to intense 46.9-nm laser pulse," *Opt. Lett.* **29**(6), 620–623 (2004).
12. D. A. G. Deacon, "Optical coating damage and performance requirements in free electron lasers," *Nucl. Instrum. Methods Phys. Res. A* **250**(1,2), 283–288 (1986).
13. E. Ziegler, G. Marot, A. K. Freung, St. Joksch, H. Kawata, L. E. Berman, and M. Iarocci, "Multilayer optics for intense synchrotron x-ray beams: recent results on their performance," *Rev. Sci. Instrum.* **63**(1), 496–500 (1992).
14. K. A. Valiev, L. V. Velikov, S. D. Dushenkov, and A. V. Mitrofanov, "Dosimetry of soft x-ray and vacuum ultraviolet radiation using the photoetching effect," *Zh. Tekh. Fiz.* **53**(3), 583–585 (1983).
15. N. V. Filippov, T. I. Fillipova, I. V. Khutoretskaia, V. V. Mialton, and V. P. Vinogradov, "Megajoule scale plasma focus as efficient x-ray source," *Phys. Lett. A* **A211**(3), 168–171 (1996).
16. B. Rus, T. Mocek, A. R. Prag, M. Kozlova, M. Hudecek, G. Jamelot, A. Carillon, D. Ros, J. C. Lagron, D. JoyeuX, and D. Phalippou, "Multi-millijoule, deeply saturated x-ray laser at 21.2 mn for applications in plasma physics," *Plasma Phys. Controlled Fusion* **44**(12B), B207–223 (2002).
17. R. Sobierajski, J. Krzywinski, A. Andrzejczuk, U. Hahn, R. Treusch, M. Jurek, D. Klinger, R. Nietubyc, J. B. Pelka, H. Reniewicz, M. Sikora, and W. Sobala, "Experimental station to study the interaction of intense femtosecond vacuum ultraviolet pulses with matter at TTF1 free electron laser," *Rev. Sci. Instrum.* **76**(1), 013909 (2005).
18. L. Juha, A. R. Präg, J. Krasa, A. Cejnarova, B. Kralikova, J. Skala, D. Chvostova, J. Krzywinski, A. Andrejczuk, M. Jurek, D. Klinger, R. Sobierajski, H. Fiedorowicz, A. Bartnik, L. Pína, J. Kravarik, P. Kubes, Y. L. Bakshaev, A. S. Chernenko, V. D. Korolev, V. I. Tumanov, M. I. Ivanov, M. Scholz, L. Ryc, K. Tomaszewski, R. Viskup, and F. P. Boody, "Ablation of organic polymers and elemental solids induced by intense XUV radiation," *AIP Conf. Proc.* **641**, 504–509 (2002).
19. R. Sobierajski, J. Krzywinski, A. Andrejczuk, B. Faatz, F. Felten, S. Jacobi, L. Juha, M. Jurek, A. Kauch, D. Klinger, J. B. Pelka, E. Saldin, E. Schneidmiller, M. Sikora, B. Steeg, and M. Yurkov, "Structural changes at solid surfaces irradiated with femtosecond, intense XUV pulses generated by TTF-FEL," *Proc. 24th Intl. Free Electron Laser Conf. 9th FEL Users Workshop*, K. J. Kim, S. V. Milton, and E. Gluskin, Eds., pp. II77–78, Elsevier, Amsterdam (2003).
20. L. Juha, J. Krása, A. Cejnarová, D. Chvostová, V. Vorlíček, J. Krzywinski, R. Sobierajski, A. Andrejczuk, M. Jurek, D. Klinger, H. Fiedorowicz, A. Bartnik, M. Pfeifer, P. Kubát, L. Pína, J. Kravárik, P. Kubeš, Y. L. Bakshaev, A. S. Chernenko, V. D. Korolev, M. I. Ivanov, M. Scholz, L. Ryc, J. Feldhaus, J. Ullschmied, and F. P. Boody, "Ablation of various materials with intense XUV radiation," *Nucl. Instrum. Methods Phys. Res. A* **507**(1,2), 577–581 (2003).
21. D. Bäuerle, *Laser Processing and Chemistry*, 3rd Ed., Springer, Berlin (2000).
22. R. Srinivasan, E. Sutcliffe, and B. Braren, "Ablation and etching of polymethylmethacrylate by very short (160 fs) ultraviolet (308 nm) laser-pulses," *Appl. Phys. Lett.* **51**(16), 1285–1287 (1987).
23. S. Küper and M. Stuke, "Femtosecond UV excimer laser ablation," *Appl. Phys. B* **44**(4), 199–204 (1987).
24. J. J. Rocca, "Table-top soft x-ray lasers," *Rev. Sci. Instrum.* **70**(10), 3799–3827 (1999).
25. H. Daido, "Review of soft x-ray laser researches and developments," *Rep. Prog. Phys.* **65**(10), 1513–1576 (2002).
26. E. Plönjes, J. Feldhaus, and T. Möller, "Taking free-electron lasers into the x-ray regime," *Phys. World* **16**(7), 33–37 (2003).
27. R. Treusch and J. Feldhaus, "SASE free electron lasers as short wavelength coherent sources—From first results at 100 nm to a 1 Å x-ray laser," *Eur. J. Phys.* **D26**(1), 119-122 (2003).
28. G. J. Tallents, "The physics of soft x-ray lasers pumped by electron collisions in laser plasmas," *J. Phys. D* **36**(15), R259–R276 (2003).
29. L. Juha, J. Krzywinski, A. Andrejczuk, M. Bittner, J. Feldhaus, J. B. Pelka, R. Sobierajski, B. Steeg, and A. Wawro, "Laser-induced periodic surface structures (LIPSS) produced by short-wavelength, fast beam of TTF1 FEL," *HASYLAB Annu. Rep., Part I*, pp. 763–764 (2003).
30. H. Fiedorowicz, A. Bartnik, L. Juha, K. Jungwirth, B. Kralikova, J. Krasa, P. Kubat, M. Pfeifer, L. Pina, P. Prchal, K. Rohlena, J. Skala, J. Ullschmied, M. Horvath, and J. Wawer, "High-brightness laser plasma soft x-ray source using a double-stream gas puff target irradiated with the prague asterix laser system (PALS)," *J. Alloys Compd.* **362**(1,2), 67–70 (2004).
31. J. Arthur, "Status of the LCLS X-ray FEL program," *Rev. Sci. Instrum.* **73**(3), 1393–1395 (2002).
32. A. S. Schwarz, "The European x-ray free electron laser project at DESY," *Proc. 26th Intl. Free Electron Laser Conf. 9th FEL Users Workshop*, Trieste, Italy, 29 Aug. – 3 Sept. 2004; http://xfel.desy.de/.
33. J. J. Rocca, J. Filevich, E. C. Hammarsten, E. Jankowska, B. Benware, M. C. Marconi, B. Luther, A. Vinogradov, I. Artiukov, S. Moon, and V. Shlyaptsev, "Extremely compact soft x-ray lasers based on capillary discharges," *Nucl. Instrum. Methods Phys. Res. A* **507**(1,2), 515–522 (2003).
34. B. R. Benware, A. Ozols, J. J. Rocca, I. A. Artioukov, V. V. Kondratenko, and A. V. Vinogradov, "Focusing of a tabletop soft-x-ray laser beam and laser ablation," *Opt. Lett.* **24**(23), 1714–1716 (1999).
35. V. Ayvazyan et al., "A new powerful source for coherent VUV radiation: Demonstration of exponential growth and saturation at the TTF free-electron laser," *Eur. Phys. J. D* **20**(1), 149–156 (2002).
36. B. Rus, T. Mocek, A. R. Präg, M. Kozlová, G. Jamelot, A. Carillon, D. Ros, D. JoyeuX, and D. Phalippou, "Multi-millijoule, highly coherent x-ray laser at 21 nm operating in deep saturation through double-pass amplification," *Phys. Rev. A* **66**(6), 063806-12 (2002).
37. K. Jungwirth, A. Cejnarová, L. Juha, B. Králiková, J. Krása, E. Krouský, P. Krupiková, L. Láska, K. Mašek, T. Mocek, M. Pfeifer, A. Präg, O. Renner, K. Rohlena, B. Rus, J. Skála, P. Straka, and J. Ullschmied, "The Prague asterix laser system PALS," *Phys. Plasmas* **8**(5), 2495–2501 (2001).
38. A. T. Anderson, "X-ray ablation measurements and modeling for ICF applications," PhD Thesis, Univ. California at Berkeley (1996).
39. A. T. Anderson, A. K. Burnham, M. T. Tobin, and P. F. Peterson, "Modeling and experiments of x-ray ablation of national ignition facility first wall materials," *Fusion Technol.* **30**(3), 757–763 (1996).
40. A. T. Anderson and P. F. Peterson, "Experimental methods for measuring x-ray ablation response of surfaces," *Exp. Heat Transfer* **10**(1), 51–65 (1997).
41. H. Hiraoka, "Radiation chemistry of poly(methylmethacrylate)," *IBM J. Res. Dev.* **21**(2), 121–130 (1977).
42. V. Letal, L. Juha, A. Bartnik, M. Bittner, F. P. Boody, H. Fiedorowicz, J. Krzywinski, J. Mikolajczyk, Z. Otcenasek, J. B. Pelka, R. Rakowski, K. Rohlena, and R. Sobierajski, "XUV-ABLATOR: computer code for simulation of material ablation induced by intense XUV radiation," (manuscript in preparation).
43. I. E. Ferincz, C. Toth, and J. F. Young, "Imaging characteristics of poly(methyl methacrylate) at vacuum ultraviolet wavelengths," *J. Vac. Sci. Technol. B* **14**(4), 828–832 (1997).
44. B. L. Henke, E. M. Gullikson, and J. C. Davis, "X-ray interactions-photoabsorption, scattering, transmission, and reflection at E=50-30,000 eV, Z=1-92," *At. Data Nucl. Data Tables* **54**(2), 181–342 (1993); http://www-cXro.lbl.gov/optical_constants/.
45. H. Wabnitz et al., "Multiple ionization of atom clusters by intense soft x-rays from a free-electron laser," *Nature (London)* **420**(6915), 482–485 (2002).
46. H. Wabnitz, "Interaction of intense VUV radiation from a free-

electron laser with rare gas atoms and clusters," PhD Thesis, HASYLAB / DESY, Hamburg (2003).
47. P. E. Dyer, R. J. Farley, R. Giedl, and D. M. Karnakis, "Excimer laser ablation of polymers and glasses for grating fabrication," *Appl. Surf. Sci.* **96–98**, 537-549 (1996).
48. O. Maida, N. Kohma, M. Ueno, A. Shibuya, T. Kanashima, M. Okuyama, and H. Ohashi, "Evaporation and expansion of polytetrafluoroethylene induced by irradiation of soft x-rays from spring-8 undulator," *Jpn. J. Appl. Phys., Part 1* **40**(4), 2435–2439 (2001).
49. M. C. Senaka Perera and D. J. T. Hill, "Radiation chemical yields: G values," in *Polymer Handbook*, J. Brandrup, E. H. Immergut, and E. A. Grulke, Eds., 4th ed., Vol. 1, pp. II-481-497, Wiley Interscience, New York (1999).
50. A. Holmes-Siedle and L. Adams, *Handbook of Radiation Effects*, 2nd ed., p. 569, Oxford University Press, Oxford (2002).
51. E. M. Lehockey, I. Reid, and I. Hill, "The radiation chemistry of poly(methyl methacrylate) polymer resists," *J. Vac. Sci. Technol. A* **6**(4), 828–832 (1997).
52. H. Fiedorowicz, A. Bartnik, M. Bittner, L. Juha, J. Krasa, P. Kubat, J. Mikolajczyk, and R. Rakowski, "Micromachining of organic polymers by direct photo-etching using a laser plasma x-ray source," *Microelectron. Eng.* **73-4**, 336–339 (2004).
53. A. T. Anderson, M. T. Tobin, and P. F. Peterson, "X-ray response of national ignition facility first surface materials," *Fusion Technol.* **26**(3), 804–808 (1994).
54. D. C. Eder, personal communication.
55. L. Juha, M. Bittner, D. Chvostova, J. Krasa, Z. Otcenasek, A. R. Präg, J. Ullschmied, Z. Pientka, J. Krzywinski, J. B. Pelka, A. Wawro, M. E. Grisham, G. Vaschenko, C. S. Menoni, and J. J. Rocca "Ablation of organic polymers by 46.9-nm laser radiation," *Appl. Phys. Lett.* **86**(3), 034109 (2005).
56. I. Haller, R. Feder, M. Hatzakis, and E. Spiller, "Copolymers of methyl methacrylate and methacrylic acid and their metal salts as radiation sensitive resists," *J. Electrochem. Soc.* **126**(1), 154–161 (1979).

Biographies and photographs of authors not available.